Research Square

Preprints are preliminary reports that have not undergone peer review.
They should not be considered conclusive, used to inform clinical practice,
or referenced by the media as validated information.

Transcript profiles of stria vascularis in models of Waardenburg syndrome

Linjun Chen
Chinese PLA General Hospital
Yi Wang
Chinese PLA General Hospital
Lei Chen
Chinese PLA General Hospital
Fangyuan wang
Chinese PLA General Hospital
Fei Ji
Chinese PLA General Hospital
Wei Sun
University at Buffalo - The State University of New York
Hui Zhao (huizhao301ent@163.com)
Chinese PLA General Hospital https://orcid.org/0000-0001-6879-241X
Weiju Han
Chinese PLA General Hospital

Research article

Keywords: Mitf-M gene, Waardenburg syndrome 2A, PI3K-AKT pathway, RNA-Seq, K+ ion transporter

Posted Date: October 16th, 2019

DOI: https://doi.org/10.21203/rs.2.16137/v1

License: This work is licensed under a Creative Commons Attribution 4.0 International License.
Read Full License

Version of Record: A version of this preprint was published at Neural Plasticity on August 1st, 2020. See the published version at https://doi.org/10.1155/2020/2908182.

Abstract

Background: Waardenburg syndrome is a common syndromic hereditary deafness disease caused by stria vascularis dysfunction. However, the genetic pathway affecting stria vascularis development is still not clear. In this paper, the transcript profile of stria vascularis of Waardenburg syndrome was studied using Mitf-M mutant pigs and mice models. GO analysis was performed to identify the differential gene expression caused by Mitf-M mutation.

Results: There were over than one hundred genes mainly found in tyrosine metabolism, melanin formation and ion transportations showed significant changes in both models. In addition, there were some spiced specific gene changes in the stria vascularis in the mouse and porcine models. The expression of tight junction-associated genes, including Cadm1, Cldn11, Pcdh1, Pcdh19 and Cdh24 genes , were significantly higher in porcine models compared to mouse models. Vascular-related and ion channel-related genes in the stria vascularis were also shown significantly difference between the two species. The expression of Col2a1, Col3a1, Col11a1 and Col11a2 genes were higher and the expression of Col8a2, Cd34 and Ncam genes were lower in the porcine model compared to mouse model. In both models, Trpm1, Kcnj13, and Slc45a2 genes were both affected by the Mitf-M mutation. In the pig models, the expression of Kcnn1, Clcn2 and Trpm4 genes were higher than the mouse model; whereas the expression of Trpm7, Kcnq1 and Kcnj8 genes were higher in the mouse models than the pig models. However, there was no significant difference in the morphology of the stria vascularis between these two models.

Conclusions: Our data suggests that there is a significant difference on the gene expression and function between these two models.

Background

Waardenburg syndrome is a group of genetic conditions that can cause congenital hearing loss. Using mouse models, there are more than 20 mutations in the Mitf allele [1–4], including $Mitf^{mi\text{-}vga9}$, $Mitf^{mi\text{-}bw}$ and $Mitf^{mi\text{-}ce}$, have been identified to cause hearing loss and changes in pigmentation. Although the mouse model is widely used in disease phenotypes and pathogenic mechanisms of deafness-related research [5,6], many shortcomings have also been found in studying human genetic diseases. As there is a big revolutionary difference between mouse and human, it may cause a huge biological difference in anatomy, energy metabolism and life styles [7]. For example, the developmental patterns of auditory organs are different in mice and humans: human's hearing developed before birth while mouse's hearing did not fully develop until two weeks after birth [8]. Some studies [5] found that human embryonic developmental diseases are difficult to be replicated in some of the mouse models. Therefore, different animal models, such as cattle [9], dogs [10] and pigs [11] were also necessary to be used to study genetic diseases. Pigs are precocial species with fully developed auditory system at birth. Our recent studies also found the cochlear anatomy is very similar to human [12,13]. As pigs are large-scale animals with high

reproductive efficiency and economical convenience, it is a good model for study auditory genetic diseases.

The stria vascularis plays an important role in maintaining the cochlear endolymphatic potentials (EP) which is essential for the mechanical electrical conduction for the hair cells [14]. The potassium ions in the scala media are produced by the stria vascularis and several potassium channels and transporters, such as KCNQ1/KCNE1, KCNQ4, KCNN2, KCNJ10 and SLC12A2, are involved in maintaining the endolymphatic potentials [15–17]. For example, Marcus [18] reported that Kcnj10 knockout can decrease EP value from +80 mV to 1 mV, and the K^+ concentration decrease from 110 mM to 60 mM in their mouse models. In our previous studies, we found that Mitf-M knockout can decrease the EP to 18 mV in the mouse model [19]. In the Mitf knockout pig model, we found that the Mitf mutation caused value of EP dropped from +78 mV to +3 mV, which was lower than the mouse model [12]. In a wild type pig, the potassium concentration in the endolymph was 142 mM higher than those in the perilymph. Our previous study found in the Mitf mutant pigs, the potassium concentration dropped to 0 mM [12]. We expect that there may be different genes in maintaining the EP in mice and pigs, and the mutation of Mitf gene may cause different change in potassium channels. To answer these questions, this study attempted to detect changes in the genetic profiles of these two species caused by Mitf-M gene mutation in RNA transcriptome level. As most of the current researches only use mouse models, this paper will further detect the RNA transcriptome difference in the stria vascularis between the large animals and mouse models.

Results

- Gene expression changes caused by Mitf-M mutation

The activation of different genes in the stria vascularis of pigs and mice caused by the Mitf-M mutation compared to their W/T controls were screened using the DESeq package software. The conditions for screening differential genes were corrected P-value < 0.05. The intersections of the differential genes in the pigs and mice were obtained using the Venn Diagrams. The results were shown in the Table 1. There were 14 common differential genes between the Mitf mutant animals and the controls. There were 177 specific differential genes in mouse model and 99 specific differential genes in pig models.

The GO analysis and the KEGG pathway analysis were performed on the David Database (adjusted p value <0.05). The results were shown in Figure 2. The main pathway caused by Mitf mutation was the KEGG pathway, enriched in the tyrosine metabolism (mmu00350) and the melanogenesis pathway (Melanogenesis, mmu04916). The GO analysis was mainly enriched in the biological process of ion transport (ion transport, GO: 0006811) and the integral component of plasma membrane (GO: 0005887).

2. Stria vascularis specific ion transport-related gene analysis.

Ion transport-related genes were extracted from RNA transcriptome data from the normal and Mitf-m mutant pigs and mice samples for cluster analysis. The results showed many ion transport-related genes were highly expressed in both species through MeV cluster analysis. The Mitf mutation were co-affected with *Trpm1, Kcnj13* and *Slc45a2* genes in both species. There were significant differences in ion channel regulation between pigs and mice. The expression of *Kcnn1, Clcn2* and *Trpm4 genes* were higher in pigs than those genes in the mice, whereas the expression of *Trpm7, Kcnq1* and *Kcnj8* genes were found higher in mice compared to the pigs.

3. The specific tight junction-associated genes in the stria vascularis

The tight junction-associated genes were extracted from the RNA transcriptome data from the Mitf mutant and normal pigs/mice for cluster analysis. The expression of tight junctions in the stria vascularis of the two species were different. The *Cadm1, Cldn11, Pcdh1, Pcdh19* and *Cdh24* genes expressed higher inpigs compared to those genes in mice; whereas *Ncam, Cldn6, Cldn9* and *Cldn14* genes expressed higher in mice compared to pigs.

- Stria vascularis specific vascular development-related genes.

Extracted vascular development-related genes from the RNA transcriptome data of the Mitf mutant and normal pigs/mice were used for cluster analysis. There was a significant difference in the vascular developmental genes in the stria vascularis between these two species. The *Col2a1, Col3a1, Col11a1, Col11a2* genes expressed higher in the pigs than the mice; whereas the *Col8a2, Cd34, Ncam* genes expressed higher in the mice compared to the pigs.

Discussion

This paper studies Mitf-M mutation on gene expression changes in the cochlea. Mitf has many subtypes [22], in which type M is specifically expressed in melanocytes[23], by direct association with related pigmentases such as tyrosinase (Tyr), dopachrome tautomerase (Dct), endothelin receptor type B (Ednrb), solute carrier family 45 member 2 (Slc45a2), regulating the survival, migration and differentiation of melanocytes[24]. Among them, Mitf-M gene [23,25,26] plays a key role in regulating tyrosine metabolic pathway and melanin production, mainly regulating downstream pigment-related enzymes such as Tyr, Dct, Tyrp1, etc. Mitf-M also controls cytoskeleton and intercellular tight protein to regulate morphology and migration of melanocytes. In this study, we found the main gene pathway caused by the Mitf-M mutation is on ion transport pathway, including the tyrosine, acid metabolism and melanin formation pathways, in the cochlear stria vascularis of both mice and pigs. Our data are consistent with previous reports.

Our previous studies reported that the Mitf-M gene mutation in the Waardenburg 2A pigs and mice through a deletion of the Mitf-M genes, caused melanocytes failed migrate to the cochlear stria vascularis. It can cause drops of EP and damages of cochlear hair cells. In this study, we also identified a significant decrease of the K^+ channel-associated genes, i.e., *Trpm1, Kcnj13, Slc45a2,* and *Kcnj10.* From

our RNA-seq sequencing analysis, *Clcnka* and *Kcnj15* genes showed a significant difference in pig models; whereas the *Kcnq4, Kcnn4, Kcne1* and *Kcnj2* genes are affected mainly in the mouse models. KCNJ13 (KIR7.1) and KCNJ10 (KIR4.1) are belong to the inward rectifier potassium channel category. KCNJ10 is known as the key channel of potassium transport. It has been deeply studied in deafness-related diseases, and its deletion can lead to the reduction of EP and potassium ion concentration [18,27–32]. However, Kcnj13, Trpm1, Slc45a2 were rarely reported in auditory researches. In addition, TRPM1 is a non-selective voltage-gated cation channel in the transient receptor potential (TRP) family and the *Mitf* mutation can lead to the deletion of *Trpm1* [33]. SLC45A2 is a cross-mediated melanin synthesis in membrane transporter [34,35], which is regulated by *Mitf* via the cAMP pathway through *Tyr* and *Dct* genes, the major pigment-related genes [36,37].

The stria vascularis transcriptome data of the two species indicated that Mitf-M played an important role in regulating the expression of the *Trpm1, Kcnj13, Slc45a2* and *Kcnj10* genes in thestria vascularis. In both species, Mitf-M may play an important role in the auditory develop and maintain the EP in the cochlea. Although there were huge biological differences between pigs and mice, we found that common gene changes in both species caused by Mitf-M. Mitf-M mutation induced a significant change in *Clcn2, Kcnn1, Trpm4* genes in the both models. CLCN2 [17] is an important component of chloride channel, which coordinates potassium and chloride exchanges. The function of KCNN1 has not been reported in the inner ears. KCNN1 belongs to the calcium ion-mediated potassium channels and plays an important role in the regulation of neural inflammation and nerve aging by microglia [38], In mice, *Kcnq1, Trpm7,* and *Kcnj8* were significantly affected. KCNQ1 is a calcium ion-dependent potassium channel [39]. When Kcnq1 is deleted, it will cause degeneration of the outer hair cells, which is clinically characterized as Jervell and Lange-Nielsen syndrome, one condition that causes profound hearing loss from birth and a disruption of the heart's normal rhythm. KCNE1 and KCNQ1, are important potassium-secreting channels in the stria vascularis marginal cells [31,39,40]. KCNE1 regulates KCNQ1 expression and increases ion transport [41].

The tight junctions and vascular endothelial cells are important components of the blood labyrinth barrier as well as ion channels [42–46]. Our cluster analysis of the RNA transcriptome data from both pigs and mice, showed that the tight junctions were significantly different in the stria vascularis of these two species. The expression of *Cadm1, Cldn11, Pcdh1, Pcdh19* and *Cdh24;* were found higher in pigs compared to mice; whereas the expression of *Ncam, Cldn6, Cldn9* and *Cldn14* genes were higher in mice compared to pigs.Cluster analysis of vascular-related genes revealed that it was significantly different in the stria vascularis of the two species. The higher expression in pigs is *Col2a1, Col3a1, Col11a1* and *Col11a2;* whereas the expression of *Col8a2, Cd34* and *Ncam* genes were higher in mice compared to pigs. The differences between two species' evolutionary relationship, living habits and anatomy, may result in significant differences in these gene expressions [46–48]. It is more suitable to choose animal model closer to humans to study auditory related diseases.

Conclusions

Our data suggests that there is a significant difference on the gene expression and function between these two models.

Abbreviations

WS, Waardenburg syndrome; EP, endolymphatic potentials; Tyr, tyrosinase; Dct, dopachrome tautomerase; Ednrb, endothelin receptor type B; Slc45a2, solute carrier family 45 member 2; TRP, transient receptor potential.

Methods

- Animals

Both Mitf mutant and normal pigs and mice have been used in this experiment. The generation of the Mitf mutant pigs and mice have been described in our previous publications [11,19]. The experimental protocols were approved by the ethics committee of the Chinese PLA Medical School. All animal surgeries and procedures were conducted according to the guidelines of the Ethics Committee of the PLA General Hospital and approved by the Animal Ethics Committee of the Institute of Zoology, Chinese Academy of Sciences. All of the pigs were provided by the institute of Zoology, Chinese Academy of Sciences. At the end, the sows were over-anesthetized with increasing the most amount of inhaled anesthesia, 0.5 ml/min isofurane until breathing and the heartbeat stopped. There was no pain in the entire process. Animal carcasses were handed over to the management department for unified treatment approach.

- RNA Isolation From Stria Vascularis Tissue

Tissues of the stria vascularis of pigs were obtained from four normal pigs and four Mitf mutant pigs at E85 of embryonic stage. The tissues of stria vascularis of mice were obtained from ten normal mice and ten Mitf mutant mice at postnatal 30 days. The total RNA of these tissues were extracted separately using Trizol reagent (Invitrogen, CA, USA) following the manufacturer's protocol. The quantity, purity and integrity of the collected total RNA were analyzed with NanoPhotometer® spectrophotometer (IMPLEN, CA, USA), a Bioanalyzer 2100 and RNA Nano 6000 Assay Kit (Agilent, CA, USA). Approximately 4 μg of total RNA was used for the RNA sample preparations.

- Library Construction and Sequencing

The NEBNext® Ultra TM RNA Library Prep Kit for Illumina® (NEB, USA) was used for the sequencing library preparation, which was conducted with an Illumina HiSeq TM 2000 system following the manufacturer's recommended protocol (Illumina Company Ltd, San Diego, CA, USA).

RNA-Seq Reads Mapping

The reference genome and gene model annotation files were obtained from Genome Web (http://asia.ensembl.org/index.html). Index of the reference genome was built using Hisat2 software (v2.0.5) and the paired-end clean reads were aligned to the reference genome. A database of potential splice junctions was built and confirmed by comparing the previously unmapped reads against the database of putative junctions. The aligned read files were processed by Cufflinks software, which used the normalized RNA-seq fragment counts to measure the relative abundances of the transcriptome. The unit of measurement was fragmented per kilobase of exons per million fragments mapped (FPKM).

Gene Ontology (GO) and Pathway Enrichment Analysis of DEGs

Differential expression analysis of Mitf-M mutant and normal pigs/mice were performed using the DEseq R package. Using the adjusted P values 0.05 and setting absolute fold change of 2 as the threshold for significantly differential expression. Using Gene Ontology (GO) and KEGG to analyze high-throughput genome and transcriptome data in the DAVID database [20,21], which is an important online tool for these analyses. The DEGs list was uploaded to the DAVID analysis tool and $P < 0.05$ was considered statistically significant. The DEGs was uploaded to the MeV software (https://sourceforge.net/projects/mev-tm4/) to get the relevant heat map.

Transcriptome annotation:

Latest annotation file: sus scrofa ensembl release 94.

Latest gene version: Sus scrofa 11.1 (GCA_ 000003025.6).

Mus musculus: ensemble release 68.

Mus musculus: NCBIM38 (GCA_000001635.8).

Data analysis:

Ensemble database: http://asia.ensembl.org/Sus_scrofa/Info/Index;

DVAID data processing website: https://david.ncifcrf.gov/summary.jsp;

Venn diagram: http://bioinformatics.psb.ugent.be/webtools/Venn/.

The transmission electron microscopy (TEM)

To prepare samples for TEM examination, the stria vascularis were washed with 0.1 M PBS and then post-fixed in 1% osmium tetroxide and then dehydrated by a series of ethanol before embedded in plastic Agar 100 resin. After polymerization, the stria vascularis was cut into ultrathin sections (3 μm), stained with toluidine blue, were mounted on 0.7% formvar coated copper grids, contrasted by 0.5% uranyl acetate and lead citrate, then examined under a transmission electron microscopy (Philips Tecnai10).

Declarations

Ethics approval and consent to participate

All animal surgeries and procedures were conducted according to the guidelines of the Ethics Committee of the PLA General Hospital and approved by the Animal Ethics Committee of the Institute of Zoology, Chinese Academy of Sciences.

Consent to publish

Not applicable.

Availability of data and material

All data generated or analysed during this study are included in this published article. All authors who would like support with depositing and managing their data can also submit datasets to Springer Nature as part of our publisher's Data Support Services.

Competing interests

The authors declare that they have no competing interests.

Funding

This work was supported by grants from the National Key R&D Program of China (2017YFA0104702), National Natural Science Foundation of China (NSFC #81670940;817709992), The clinical support fund of General Hospital of the PLA (2017FC-TSYS–2016), The Youth cultivation project of military medical science (16QNP133), Medical big data research and development project of PLA general hospital (2018MBD–015), and the capital health research and development of special project (2016–1–5014).

Authors' contributions

CLJ, WY, and CL performed the investigation and interpreted the data. WFY, JF, and SW performed the histological examination. Moreover, ZH and HWJ were the major contributors in writing the manuscript. All authors read and approved the final manuscript.

Acknowledgements

Not applicable.

References

[1] Tachibana M, Kobayashi Y, Matsushima Y. Mouse models for four types of Waardenburg syndrome[J]. Pigment Cell Res, 2003, 16(5): 448–54.

[2] Zimring D C, Lamoreux M L, Millichamp N J, et al. Microphthalmia cloudy-eye (mi(ce)): a new murine allele[J]. J Hered, 1996, 87(4): 334–8.

[3] Tachibana M, Hara Y, Vyas D, et al. Cochlear disorder associated with melanocyte anomaly in mice with a transgenic insertional mutation[J]. Mol Cell Neurosci, 1992, 3(5): 433–45.

[4] Steingrimsson E, Copeland N G, Jenkins N A. Melanocytes and the microphthalmia transcription factor network[J]. Annu Rev Genet, 2004, 38: 365–411.

[5] Ohlemiller K K, Jones S M, Johnson K R. Application of Mouse Models to Research in Hearing and Balance[J]. J Assoc Res Otolaryngol, 2016, 17(6): 493–523.

[6] Smithies O. Animal models of human genetic diseases[J]. Trends Genet, 1993, 9(4): 112–6.

[7] Wang D. Evolution and restoration of structures and functions of the human central nervous system—A review[J]. Journal of Neurorestoratology, 2015, 1(1): 60–70.

[8] Tritsch N X, Bergles D E. Developmental Regulation of Spontaneous Activity in the Mammalian Cochlea[J]. The Journal of Neuroscience, 2010, 30(4): 1539–1550.

[9] Philipp U, Lupp B, Momke S, et al. A MITF mutation associated with a dominant white phenotype and bilateral deafness in German Fleckvieh cattle[J]. PLoS One, 2011, 6(12): e28857.

[10] Tsuchida S, Takizawa T, Abe K, et al. Identification of microphthalmia-associated transcription factor isoforms in dogs[J]. Vet J, 2009, 182(2): 283–93.

[11] Chen L, Guo W, Ren L, et al. A de novo silencer causes elimination of MITF-M expression and profound hearing loss in pigs[J]. BMC Biol, 2016, 14: 52.

[12] Guo W, Yi H, Ren L, et al. The morphology and electrophysiology of the cochlea of the miniature pig[J]. Anat Rec (Hoboken), 2015, 298(3): 494–500.

[13] Lovell J M, Harper G M. The morphology of the inner ear from the domestic pig (Sus scrofa)[J]. J Microsc, 2007, 228(Pt 3): 345–57.

[14] Dror A A, Avraham K B. Hearing Impairment: A Panoply of Genes and Functions[J]. Neuron, 2010, 68(2): 293–308.

[15] Zdebik A A, Wangemann P, Jentsch T J. Potassium ion movement in the inner ear: insights from genetic disease and mouse models[J]. Physiology (Bethesda), 2009, 24: 307–16.

[16] Jin Z. Cochlear homeostasis and its role in genetic deafness[J]. Journal of Otology, 2009, Vol. 4 (No. 1).

[17] Lang F, Vallon V, Knipper M, et al. Functional significance of channels and transporters expressed in the inner ear and kidney[J]. Am J Physiol Cell Physiol, 2007, 293(4): C1187–208.

[18] Marcus D C, Wu T, Wangemann P, et al. KCNJ10 (Kir4.1) potassium channel knockout abolishes endocochlear potential[J]. Am J Physiol Cell Physiol, 2002, 282(2): C403–7.

[19] Liu H, Li Y, Chen L, et al. Organ of Corti and Stria Vascularis: Is there an Interdependence for Survival? [J]. PLoS One, 2016, 11(12): e0168953.

[20] Huang Da W, Sherman B T, Lempicki R A. Systematic and integrative analysis of large gene lists using DAVID bioinformatics resources[J]. Nat Protoc, 2009, 4(1): 44–57.

[21] Dennis G, Jr., Sherman B T, Hosack D A, et al. DAVID: Database for Annotation, Visualization, and Integrated Discovery[J]. Genome Biol, 2003, 4(5): P3.

[22] Takeda K, Yasumoto K, Kawaguchi N, et al. Mitf-D, a newly identified isoform, expressed in the retinal pigment epithelium and monocyte-lineage cells affected by Mitf mutations[J]. Biochim Biophys Acta, 2002, 1574(1): 15–23.

[23] Chen T, Zhao B, Liu Y, et al. MITF-M regulates melanogenesis in mouse melanocytes[J]. J Dermatol Sci, 2018, 90(3): 253–262.

[24] Michael H T, Graff-Cherry C, Chin S, et al. Partial Rescue of Ocular Pigment Cells and Structure by Inducible Ectopic Expression of Mitf-M in MITF-Deficient Mice[J]. Invest Ophthalmol Vis Sci, 2018, 59(15): 6067–6073.

[25] Levy C, Khaled M, Fisher D E. MITF: master regulator of melanocyte development and melanoma oncogene[J]. Trends Mol Med, 2006, 12(9): 406–14.

[26] Vance K W, Goding C R. The transcription network regulating melanocyte development and melanoma[J]. Pigment Cell Res, 2004, 17(4): 318–25.

[27] Locher H, De Groot J C, Van Iperen L, et al. Development of the stria vascularis and potassium regulation in the human fetal cochlea: Insights into hereditary sensorineural hearing loss[J]. Dev Neurobiol, 2015, 75(11): 1219–40.

[28] Chen J, Zhao H B. The role of an inwardly rectifying K(+) channel (Kir4.1) in the inner ear and hearing loss[J]. Neuroscience, 2014, 265: 137–46.

[29] Yang H, Xiong H, Huang Q, et al. Compromised potassium recycling in the cochlea contributes to conservation of endocochlear potential in a mouse model of age-related hearing loss[J]. Neurosci Lett, 2013, 555: 97–101.

[30] Wangemann P, Itza E M, Albrecht B, et al. Loss of KCNJ10 protein expression abolishes endocochlear potential and causes deafness in Pendred syndrome mouse model[J]. BMC Med, 2004, 2: 30.

[31] Wangemann P. K+ cycling and the endocochlear potential[J]. Hear Res, 2002, 165(1–2): 1–9.

[32] Wangemann P. K(+) cycling and its regulation in the cochlea and the vestibular labyrinth[J]. Audiol Neurootol, 2002, 7(4): 199–205.

[33] Miller A J, Du J, Rowan S, et al. Transcriptional regulation of the melanoma prognostic marker melastatin (TRPM1) by MITF in melanocytes and melanoma[J]. Cancer Res, 2004, 64(2): 509–16.

[34] Inagaki K, Suzuki T, Ito S, et al. Oculocutaneous albinism type 4: six novel mutations in the membrane-associated transporter protein gene and their phenotypes[J]. Pigment Cell Res, 2006, 19(5): 451–3.

[35] Newton J M, Cohen-Barak O, Hagiwara N, et al. Mutations in the human orthologue of the mouse underwhite gene (uw) underlie a new form of oculocutaneous albinism, OCA4[J]. Am J Hum Genet, 2001, 69(5): 981–8.

[36] Hoek K S, Schlegel N C, Eichhoff O M, et al. Novel MITF targets identified using a two-step DNA microarray strategy[J]. Pigment Cell Melanoma Res, 2008, 21(6): 665–76.

[37] Du J, Fisher D E. Identification of Aim–1 as the underwhite mouse mutant and its transcriptional regulation by MITF[J]. J Biol Chem, 2002, 277(1): 402–6.

[38] Dolga A M, Culmsee C. Protective Roles for Potassium SK/K(Ca)2 Channels in Microglia and Neurons[J]. Front Pharmacol, 2012, 3: 196.

[39] Mittal R, Aranke M, Debs L H, et al. Indispensable Role of Ion Channels and Transporters in the Auditory System[J]. Journal of Cellular Physiology, 2017, 232(4): 743–758.

[40] Wilms V, Koppl C, Soffgen C, et al. Molecular bases of K(+) secretory cells in the inner ear: shared and distinct features between birds and mammals[J]. Sci Rep, 2016, 6: 34203.

[41] Strutz-Seebohm N, Seebohm G, Fedorenko O, et al. Functional coassembly of KCNQ4 with KCNE-beta-subunits in Xenopus oocytes[J]. Cell Physiol Biochem, 2006, 18(1–3): 57–66.

[42] Bartle E I, Rao T C, Urner T M, et al. Bridging the gap: Super-resolution microscopy of epithelial cell junctions[J]. Tissue Barriers, 2018, 6(1): e1404189.

[43] Liu W, Schrott-Fischer A, Glueckert R, et al. The Human “Cochlear Battery” - Claudin–11 Barrier and Ion Transport Proteins in the Lateral Wall of the Cochlea[J]. Frontiers in Molecular Neuroscience, 2017, 10.

[44] Shi X. Pathophysiology of the cochlear intrastrial fluid-blood barrier (review)[J]. Hear Res, 2016, 338: 52–63.

[45] Kitajiri S, Katsuno T, Sasaki H, et al. Deafness in occludin-deficient mice with dislocation of tricellulin and progressive apoptosis of the hair cells[J]. Biol Open, 2014, 3(8): 759–66.

[46] Wallez Y, Huber P. Endothelial adherens and tight junctions in vascular homeostasis, inflammation and angiogenesis[J]. Biochim Biophys Acta, 2008, 1778(3): 794–809.

[47] Goncharov N V, Nadeev A D, Jenkins R O, et al. Markers and Biomarkers of Endothelium: When Something Is Rotten in the State[J]. Oxid Med Cell Longev, 2017, 2017: 9759735.

[48] Trune D R. Ion homeostasis in the ear: mechanisms, maladies, and management[J]. Current Opinion in Otolaryngology & Head and Neck Surgery, 2010, 18(5): 413–419.

Tables

Table 1. The common DEGs in pigs/mice with/without Mitf-M mutation

Gene_Name	hom_pig	het_pig	MM_mouse	WW_mouse
Tyr	0.014667	9.40833	0.00233	37.4824
Emilin2	65.6574	36.3192	52.3576	20.7289
Gsn	199.663	289.825	64.9488	223.727
Dct	1.09829	135.912	0.00277	774.431
Gpnmb	2.22801	47.8019	1.14682	86.5487
Ednrb	1.19691	12.2565	1.66075	26.9099
Ucma	198.465	285.077	256.207	523.427
Slc45a2	0.793729	24.5716	3.9E-07	45.1788
Tspan10	3.93361	18.2708	0.036796	14.1373
Clca2	68.3216	50.1806	1.59181	0.120315
Kcnj10	4.4472	14.4644	16.594	111.93
Trpm1	0.009755	14.7644	0.035483	6.75993
Plp1	0.215656	4.79304	7.71325	34.9961
Kcnj13	0.149383	14.6624	1.753	14.403

Figures

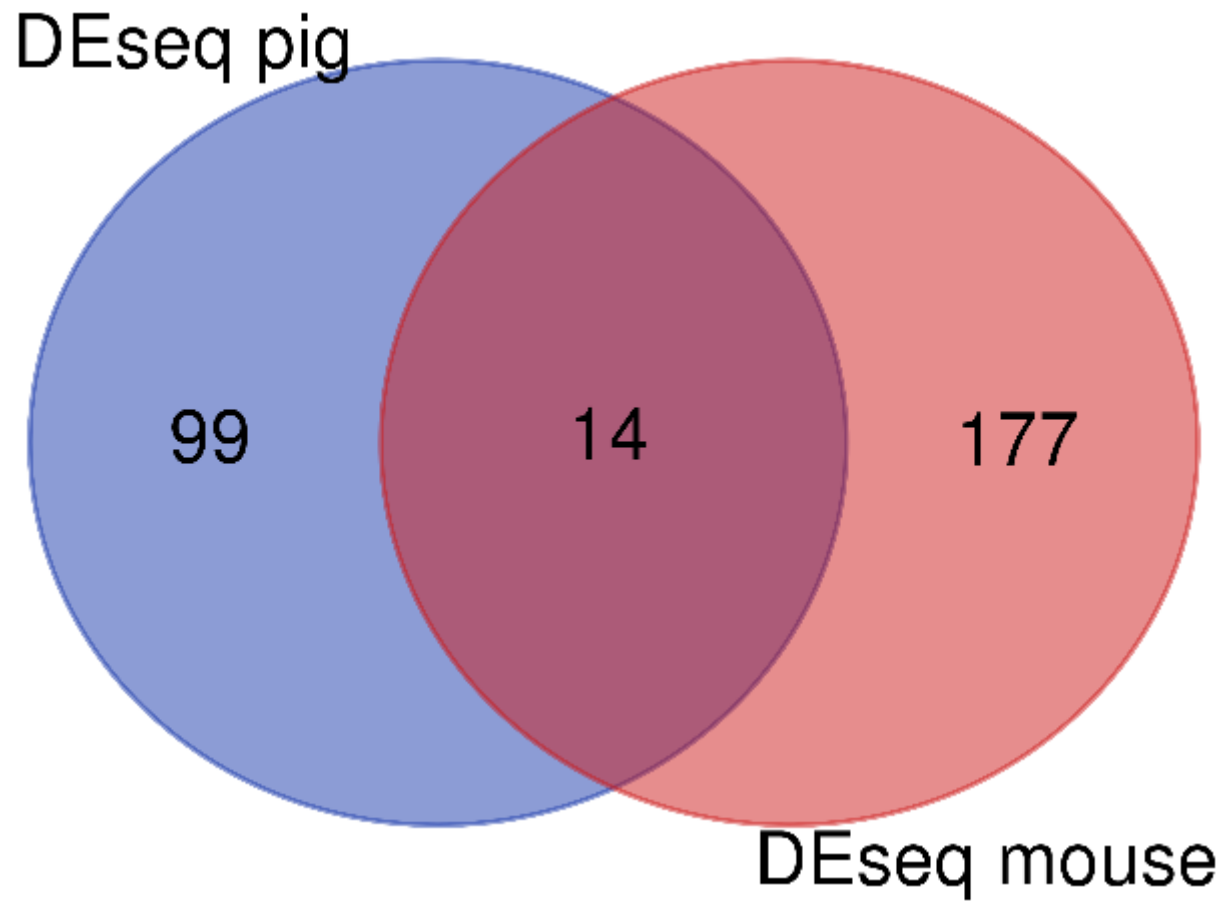

Figure 1

Venn diagram of DEGs in Mitf-M mutant and normal pigs/mice. The blue circle represents the DEGs in the Mitf-M mutant and normal pigs; the red circle represents the DEGs in the Mitf-M mutant and normal mice. The middle part represents the DEGs in the Mitf-M mutant and normal pigs/mice

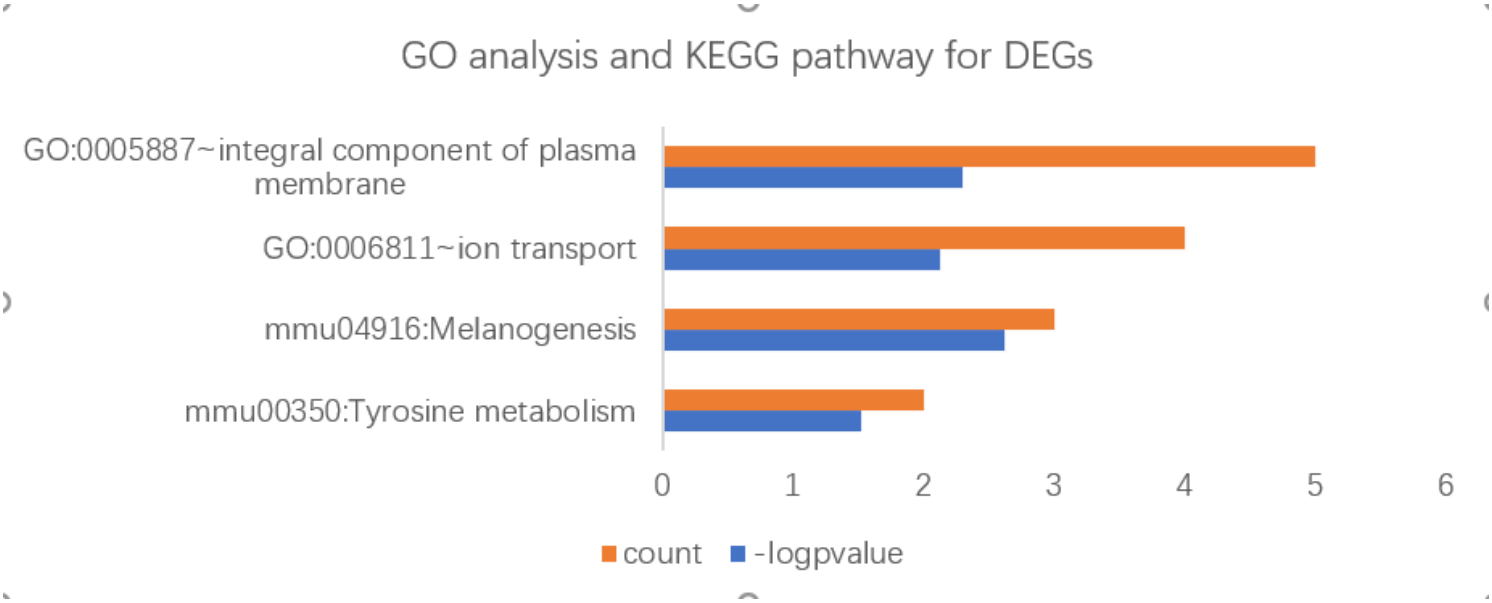

Figure 2

List of GO-terms with significant enrichment of DEGs. From top to bottom, the enrichment value decreases. The red X-axis indicates the number of unigenes in a category; The blue X-axis indicates the value of log2 (p value) in corresponding category. The Y-axis indicates the specific category.

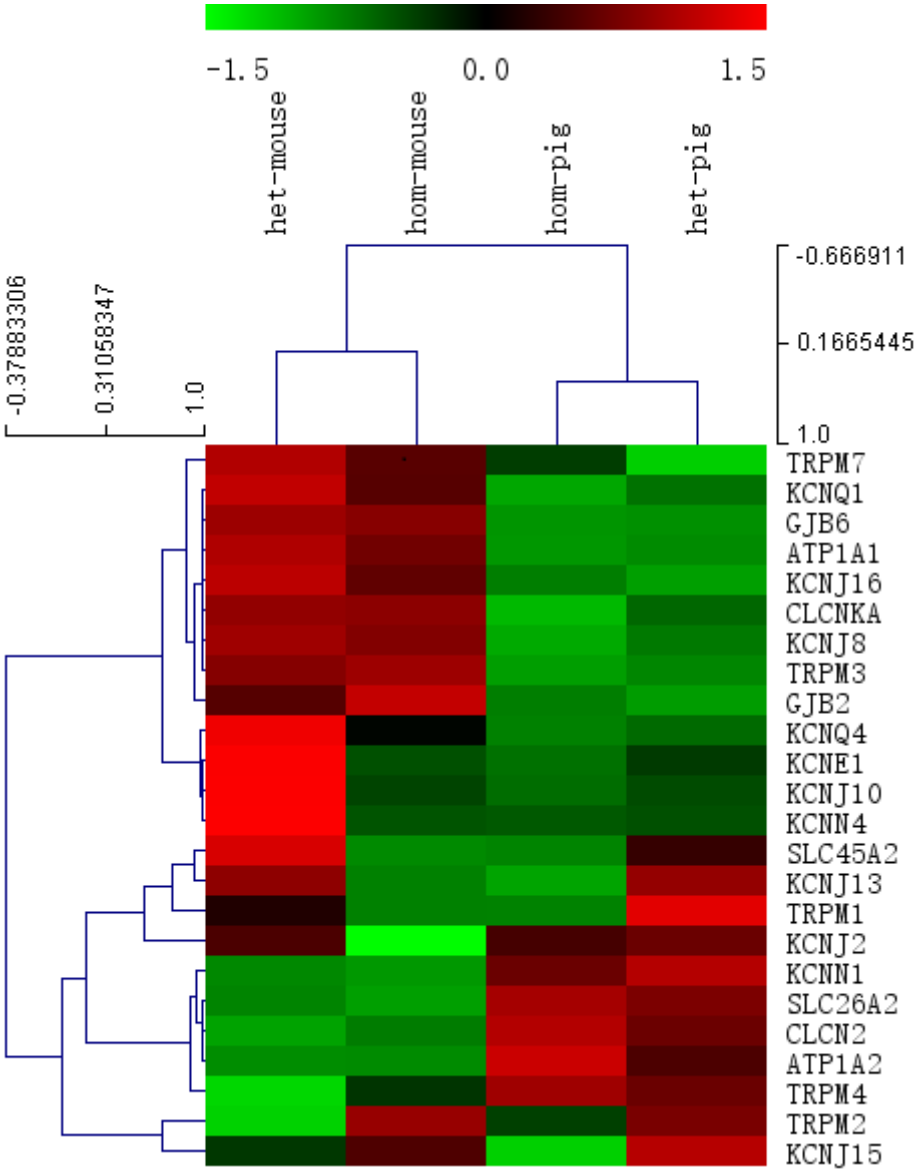

Figure 3

Ion channel relevant genes for cluster analysis heat map. Each column represents an experimental sample. Hom-mouse and het-mouse represent Mitf-M knockout mice and normal control mice. Hom-pig and het-pig represents Mitf-M mutant pigs and normal control pigs. Each row represents a gene. Different expression are shown in different colors: red represents more expression and green represents less expression.

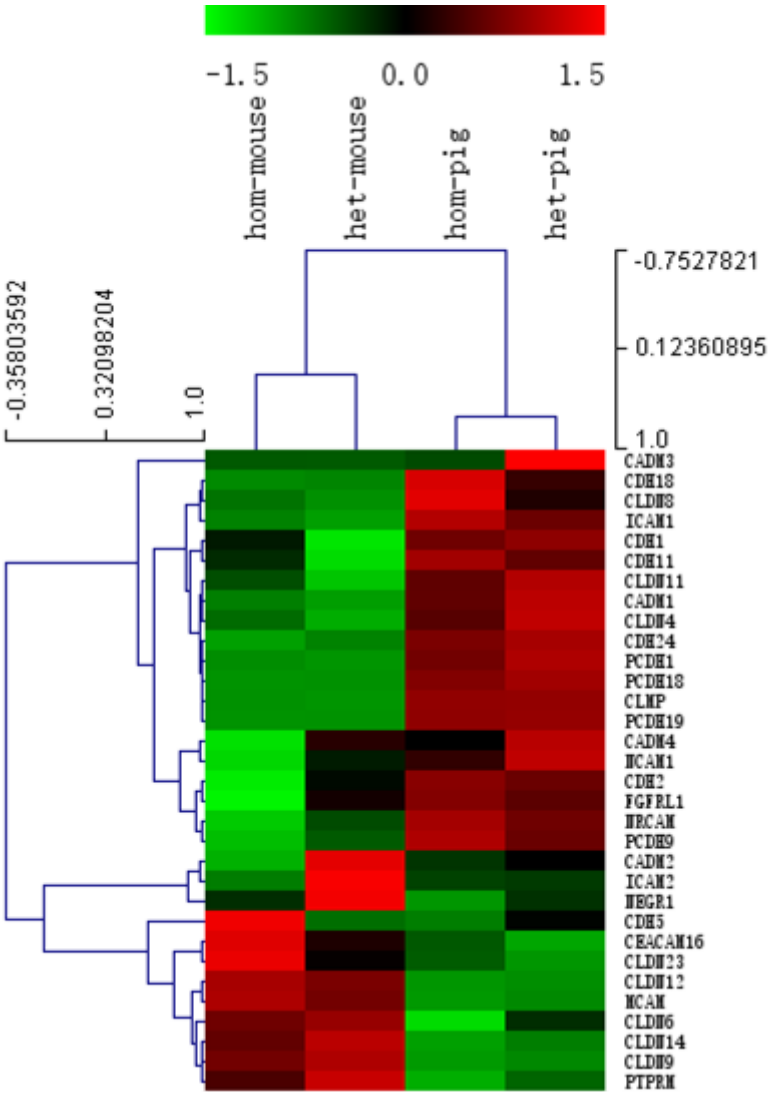

Figure 4

Tight junction relevant genes for cluster analysis heat map. Hom-mouse and het-mouse represent Mitf-M knockout mice and normal control mice. Hom-pig and het-pig represent Mitf-M mutant pigs and normal control pigs.

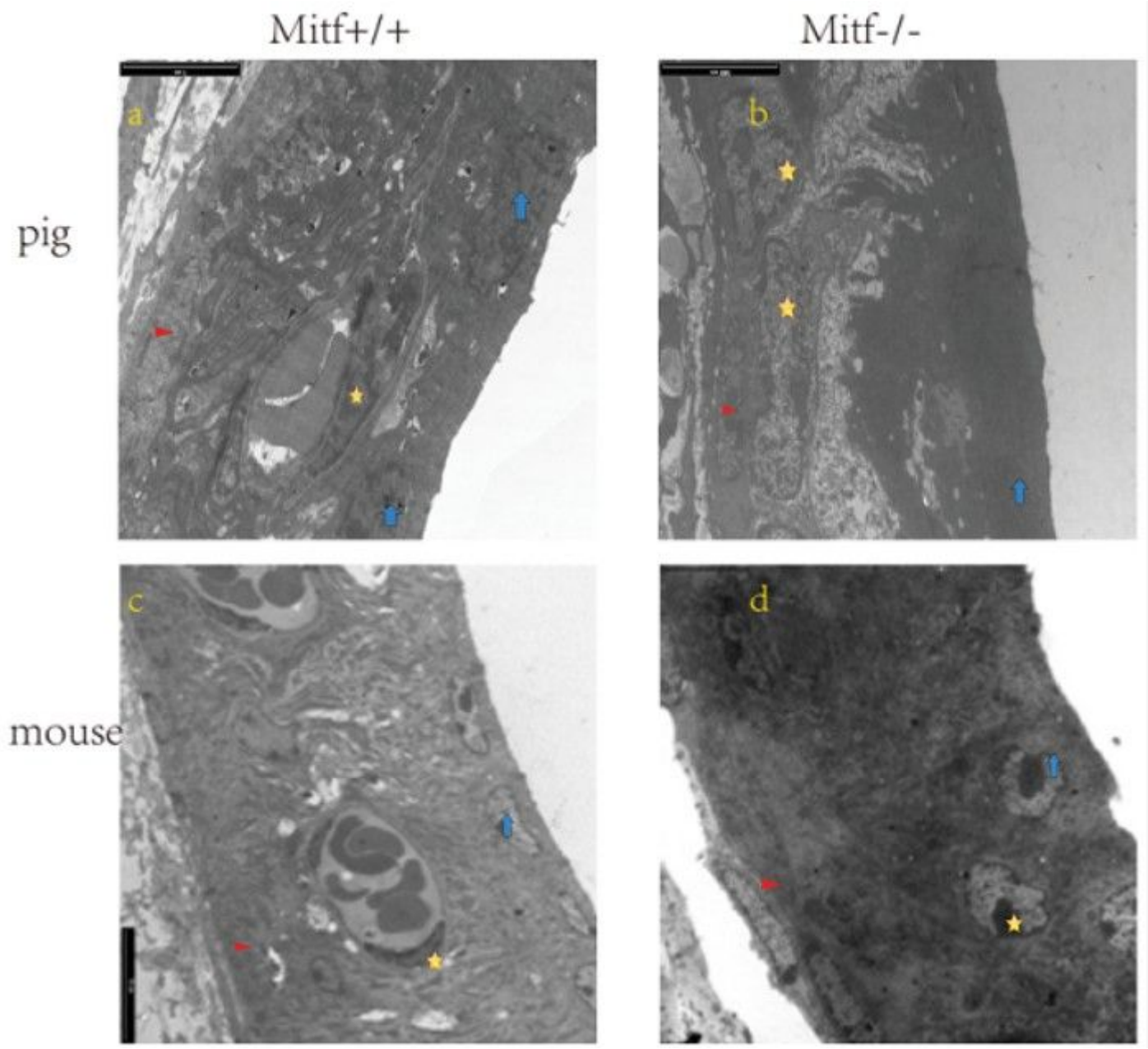

Figure 5

The SEM shows the cochlear stria vascularis of Mitf mutant and normal pigs/mice. (A) A normal pigs' stria vascularis. (B) The stria vascularis from a mutant pig. (C) The stria vascularis from a the normal mouse. (D) The stria vascularis from a mutant mouse. It was found that the marginal nuclei were intact, the cells connections were intact, the three layers of cells were clear, and the basal cells were closely connected. The red triangle marks the basal cells, the yellow pentagon marks the middle cells, and the blue arrows mark the marginal cells. The scale bar is 5 μm

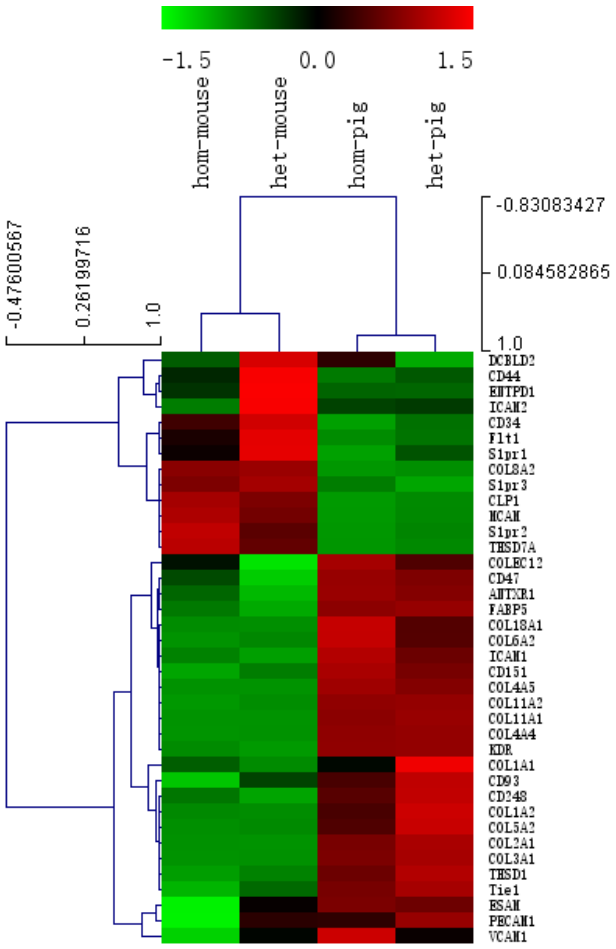

Figure 6

Heat analysis of clustering analysis of genes associated with specific vascular endothelial cell in normal and Mitf mutant pigs/mice (hom-mouse and het-mouse represent Mitf-M knockout mice and normall mice, hom-pig and het-pig represent Mitf-M mutant pigs and normal pigs).